

# Time domain spectral phase encoding/DPSK data modulation using single phase modulator for OCDMA application

Xu Wang<sup>1,\*</sup>, Zhensen Gao<sup>1</sup>, Nobuyuki Kataoka<sup>2</sup> and Naoya Wada<sup>2</sup>

<sup>1</sup>Joint Research Institute for Integrated Systems, Sch. of Engineering and Physical Sciences, Heriot-Watt University, Riccarton, Edinburgh, EH14 4AS, UK

<sup>2</sup>Photonic Network Group, New Generation Network Research Center, National Institute of Information and Communications Technology (NICT), 4-2-1, Nukui-Kitamachi, Koganei-shi, Tokyo 184-8795, Japan

\*x.wang@hw.ac.uk

**Abstract:** A novel scheme using single phase modulator for simultaneous time domain spectral phase encoding (SPE) signal generation and DPSK data modulation is proposed and experimentally demonstrated. Array-Waveguide-Grating and Variable-Bandwidth-Spectrum-Shaper based devices can be used for decoding the signal directly in spectral domain. The effects of fiber dispersion, light pulse width and timing error on the coding performance have been investigated by simulation and verified in experiment. In the experiment, SPE signal with 8-chip, 20GHz/chip optical code patterns has been generated and modulated with 2.5 Gbps DPSK data using single modulator. Transmission of the 2.5 Gbps data over 34km fiber with BER<10<sup>-9</sup> has been demonstrated successfully. The proposed scheme has simple configuration and improved flexibility that can significantly improve the data confidentiality for optical code division multiple access (OCDMA) and secure optical communication applications.

© 2010 Optical Society of America

**OCIS codes:** (060.0060) Fiber optics and optical communications; (060.5060) Phase modulation; (999.999) Encoding/decoding; (9999.999) Optical code division multiple access (999.999) secure optical communication

---

## References and links

1. P. R. Prucnal, M. A. Santoro, and T. R. Fan, "Spread spectrum fiber-optic local area network using optical processing," *J. Lightwave Technol.* **4**(5), 547–554 (1986).
2. A. Stock, and E. H. Sargent, "The role of optical CDMA in access networks," *IEEE Commun. Mag.* **40**(9), 83–87 (2002).
3. J. P. Heritage, and A. M. Weiner, "Advances in Spectral Optical Code-Division Multiple-Access," *IEEE J. Quantum Electron.* **13**(5), 1351–1369 (2007).
4. T. H. Shake, "Confidentiality performance of spectral-phase-encoded optical CDMA," *J. Lightwave Technol.* **23**(4), 1652–1663 (2005).
5. K. I. Kitayama, "Code division multiplexing lightwave networks based upon optical code conversion," *IEEE J. Sel. Areas Comm.* **16**(7), 1309–1319 (1998).
6. X. Wang, and K. Kitayama, "Analysis of beat noise in coherent and incoherent time-spreading OCDMA," *J. Lightwave Technol.* **22**(10), 2226–2235 (2004).
7. P. C. Teh, P. Petropoulos, M. Ibsen, and D. J. Richardson, "A comparative study of the performance of seven- and 63-chip optical code-division multiple-access encoders and decoders based on superstructured fiber Bragg gratings," *J. Lightwave Technol.* **19**(9), 1352–1365 (2001).
8. X. Wang, K. Matsushima, A. Nishiki, N. Wada, and K. Kitayama, "High reflectivity superstructured FBG for coherent optical code generation and recognition," *Opt. Express* **12**(22), 5457–5468 (2004).

9. H. Sotobayashi, W. Chujo, and K. Kitayama, "1.6-b/s/Hz 6.4-Tb/s QPSK-OCDM/WDM (4 OCDM  $\times$  40 WDM  $\times$  40 Gb/s) transmission experiment using optical hard thresholding," *IEEE Photon. Technol. Lett.* **14**(4), 555–557 (2002).
10. G. Cincotti, N. Wada, and K. Kitayama, "Characterization of a full encoder/decoder in the AWG configuration for code-based photonic routers—Part I: Modeling and design," *J. Lightwave Technol.* **24**(1), 103–112 (2006).
11. T. Hamanaka, X. Wang, N. Wada, A. Nishiki, and K. Kitayama, "Ten-user truly asynchronous gigabit OCDMA transmission experiment with a 511-chip SSFBG en/decoder," *J. Lightwave Technol.* **24**(1), 95–102 (2006).
12. X. Wang, N. Wada, T. Miyazaki, G. Cincotti, and K. Kitayama, "Field trial of 3-WDM  $\times$  10-OCDMA  $\times$  10.71-Gb/s asynchronous WDM/DPSK-OCDMA using hybrid E/D without FEC and optical thresholding," *J. Lightwave Technol.* **25**(1), 207–215 (2007).
13. A. M. Weiner, Z. Jiang, and D. E. Leaird, "Spectrally phase-coded O-CDMA," *J. Opt. Netw.* **6**(6), 728–755 (2007).
14. R. P. Scott, W. Cong, K. Li, V. J. Hernandez, B. H. Kolner, J. P. Heritage, and S. J. Ben Yoo, "Demonstration of an error-free 4 $\times$ 10 Gb/s multiuser SPECTS O-CDMA network testbed," *IEEE Photon. Technol. Lett.* **16**(9), 2186–2188 (2004).
15. Z. Jiang, D. Seo, S. Yang, D. E. Leaird, R. V. Roussev, C. Langrock, M. M. Fejer, and A. M. Weiner, "Four-user 10-Gb/s spectrally phase-coded O-CDMA system operating at  $\sim$  30 fJ/bit," *IEEE Photon. Technol. Lett.* **17**(3), 705–707 (2005).
16. A. Agarwal, P. Toliver, R. Menendez, T. Banwell, J. Jackel, and S. Etamad, "Spectrally Efficient Six-User Coherent OCDMA System Using Reconfigurable Integrated Ring Resonator Circuits," *IEEE Photon. Technol. Lett.* **18**(18), 1952–1954 (2006).
17. X. Wang, and N. Wada, "Spectral phase encoding of ultra-short optical pulse in time domain for OCDMA application," *Opt. Express* **15**(12), 7319–7326 (2007).
18. J. Azaña, N. K. Berger, B. Levit, and B. Fischer, "Reconfigurable generation of high-repetition-rate optical pulse sequences based on time-domain phase-only filtering," *Opt. Lett.* **30**(23), 3228–3230 (2005).
19. R. E. Saperstein, D. Panasenko, and Y. Fainman, "Demonstration of a microwave spectrum analyzer based on time-domain optical processing in fiber," *Opt. Lett.* **29**(5), 501–503 (2004).
20. S. Thomas, A. Malacarne, F. Fresi, L. Potì, A. Bogoni, and J. Azaña, "Programmable fiber-based picosecond optical pulse shaper using time-domain binary phase-only linear filtering," *Opt. Lett.* **34**(4), 545–547 (2009).
21. Z. Gao, X. Wang, N. Kataoka, and N. Wada, "Demonstration of time-domain spectral phase encoding/ DPSK data modulation using single phase modulator", LEOS Summer Topical 2009, TuA3.1, New port, CA, USA, 2009.
22. S. Anzai, M. Mieno, T. Komai, N. Wada, T. Yoda, T. Miyazaki, and K. Kodate, "Amplitude, phase, and bandwidth tunable high-resolution optical spectrum shaper and its application for optical communication systems," OFC 2008, San Diego, CA, JThA25, Feb. 2008.
23. M. Mieno, Y. Komai, N. Wada, S. Shinada, T. Yoda, T. Miyazaki, and K. Kodate, "Ultrafast Time-Spread Optical BPSK Code Label Generation and Processing Based on Variable-Bandwidth Spectrum Shaper," *IEEE Photon. Technol. Lett.* **21**(13), 860–862 (2009).

---

## 1. Introduction

Optical-code-division-multiple access (OCDMA) technique has been receiving great attention over the past decades due to its potential application in future broadband access network with unique features of fully asynchronous transmission, low latency access, simplified network management, flexible quality of service (QoS) control and potentially improved security [1-4].

Previous proposed OCDMA systems can be generally classified into two categories according to their working principle: incoherent OCDMA adopting intensity based code sequences and coherent OCDMA using phase-shifted optical sequences [5]. Among them, the coherent OCDMA performing encoding/decoding operation based on the phase and amplitude of the optical field is more attractive because of its overall superior performance over the incoherent OCDMA and the progress of compact and reliable en/decoder devices [6]. There are two kinds of coding schemes in coherent OCDMA [3]: coherent time spreading (TS) OCDMA and spectrally phase encoding time spreading (SPECTS) OCDMA. In TS-OCDMA, the

encoding/decoding is performed in time domain by directly spreading the short optical pulses. Various coding devices have been developed for this scheme including superstructured fiber Bragg grating (SSFBG) [7,8], Planar lightwave circuit (PLC) [9] and multi-port en/decoder [10], and etc. Several multiuser asynchronous OCDMA has been demonstrated with these devices [11,12]. In SPECTS OCDMA, coding is generally realized in spectral domain where different spectral component of optical pulses are encoded by different phase shift that also results in the pulse spreading in time domain [13]. Proposed SPECTS encoder/decoders include spatial lightwave phase modulator (SLPM) [14,15], micro-ring-resonator (MRR) [16] and so on. The proper decoder can fully recover the spectrum as well as the temporal waveform of the original pulse.

Recently, we have proposed a novel time domain spectral phase encoding (SPE) scheme using two dispersive fibers with opposite dispersion for stretching and compressing the ultra-short optical pulse, and a high speed phase modulator [17]. Comparing with the other SPECTS schemes, this approach is very flexible in reconfiguring the optical codes and is compatible with the fiber optical system. It is also very robust to the wavelength drift of the laser source which exhibits as a severe problem for other SPECTS schemes [17]. This technique can also find its application in high-repetition rate optical pulse generation [18], microwave spectrum analysis [19], as well as pulse shaping [20].

In this paper, we propose a novel modulation scheme based on the time domain SPE using single phase modulator to simultaneously generate optical code (OC) and modulate DPSK data. The decoding can be realized in spectral domain by using a spectral phase decoder which can be either an Array-Waveguide-Grating (AWG) [21] based device or Variable-Bandwidth-Spectrum-Shaper (VBS). We also theoretically investigate the effects of fiber dispersion, light pulse width and timing error on the coding performance in our proposed scheme. The encoding/transmission experiment has been carried out with 8-chip, 20GHz/chip optical code patterns and 2.5Gbps DPSK data, and 34km SMF.

## 2. Principle of proposed scheme

Figure 1(a) shows the principle of the SPE and DPSK data modulation with single phase modulator. An ultra-short optical pulse train with a broadband spectrum ( $\lambda_1, \lambda_2, \lambda_3, \lambda_4 \dots$ ) is directed into the SPE section, which is composed of a pair of dispersive devices with opposite dispersion sign ( $-D$  and  $+D$ ) and a high speed phase modulator (PM). The first dispersive device with dispersion value of  $-D$  is used to stretch the pulse in time domain. Different spectral components of the input pulse will spread at different time positions within one bit duration. To generate the data modulation, the PM is driven by combining the DPSK data and optical code (OC) patterns. A fixed data pattern (100...) and 4-chip OC (1101) are used as an example to show the process. The DPSK data is generated by precoding the original data (100...) into DPSK format (101...) and then combined with the OC pattern in the following way to modulate the phase of the stretched optical signal: when the DPSK data is symbol "1", the PM is driven by OC (1101...), while if the symbol is "0", the PM is driven by OC (0010...). Thus, the three bits are phase modulated by code patterns: OC (1101), OC (0010) and OC (1101), respectively. After that, the second dispersive device with opposite dispersion value of  $+D$  is used to compress the stretched pulse in time domain and generate the DPSK data modulated SPE signal.

The decoding of the generated SPE signal is same as conventional SPECTS, as shown in Fig. 1(b). The decoder with spectral phase pattern of OC is used to decode the DPSK data modulated SPE signal. The spectral components of each encoded pulse are in phase after the decoder. For symbol "1", the total phase is "OC+OC= $\pi$ ", while for symbol "0", the total phase is "OC+OC=0". Therefore, the total phase of the three bits becomes ( $\pi, 0, \pi \dots$ ) after the decoding, and the DPSK data is extracted from the SPE signal as (101...). A DPSK

demodulator with a one-bit delay interferometer followed by a balanced detector can then be used to demodulate the DPSK data and recover the original data as (100...).

In this scheme, only single phase modulator is used to realize the optical code generation and DPSK data modulation simultaneously, which provides an attractive approach to simplify the architecture of the whole OCDMA system and reduce the cost. Conventional spectral phase decoder can be used to perform the optical code recognition. Moreover, this scheme has the potential to rapidly reconfigure the optical code pattern to improve the data confidentiality, which is a unique feature than conventional OCDMA schemes. The proposed scheme can be applied for secure optical communication application.

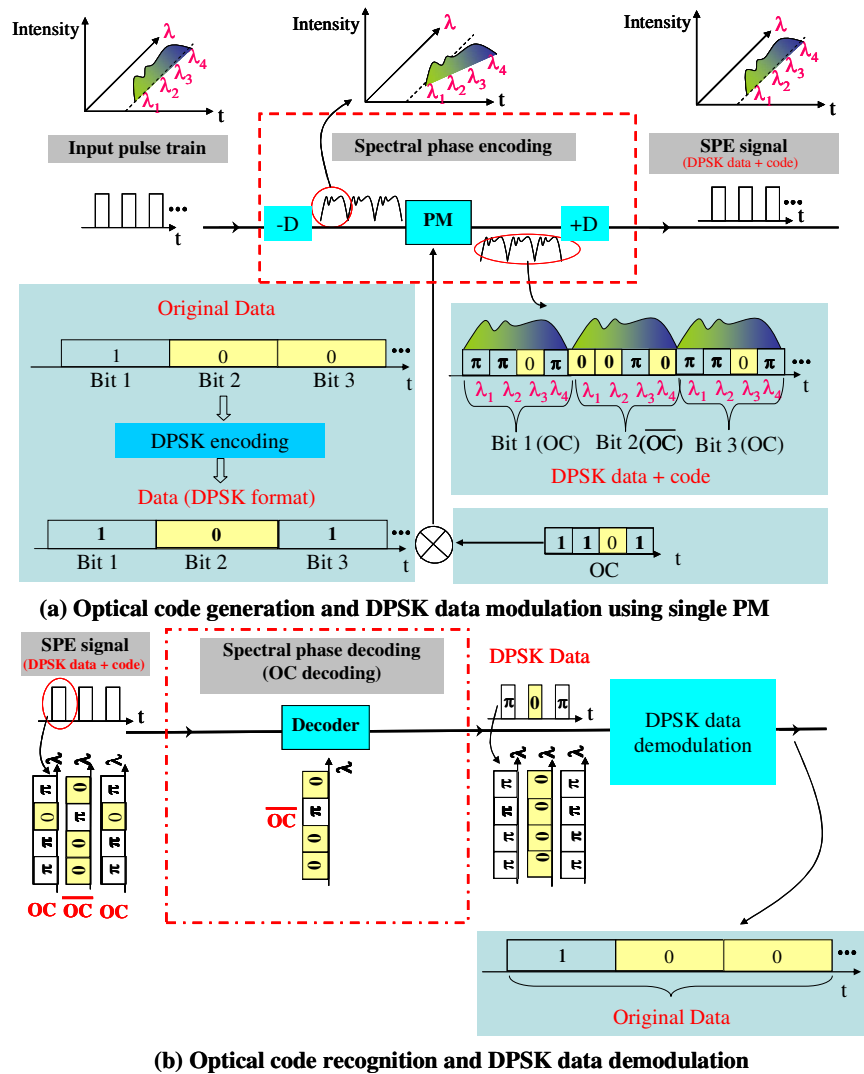


Fig. 1. Principle of the proposed scheme (a) SPE and DPSK data modulation; (b) Decoding and DPSK data demodulation

### 3. Experimental setup and simulation

Figure 2 shows the experimental setup for demonstrating the proposed scheme. In the experiment, the optical pulse source is a mode-locked-laser-diode (MLLD) producing nearly

transform-limited  $\sim 4$ ps (FWHM) Gaussian-like pulses with a repetition rate of 10GHz, spectrally centered at 1550.28nm. A Mach-Zehnder intensity modulator (IM) driven by pulse pattern generator (PPG) is used to down convert the source repetition rate to 2.5GHz.

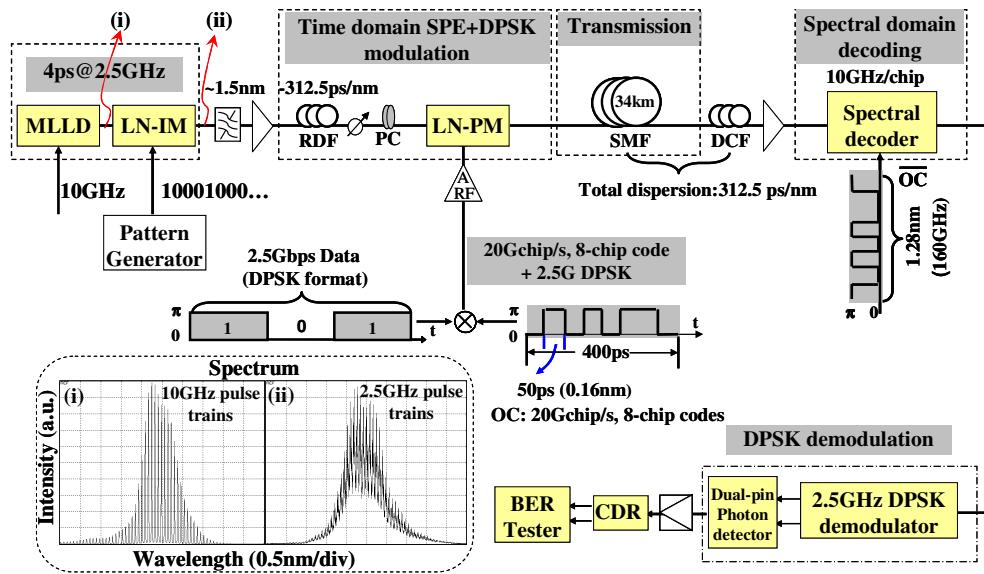


Fig. 2. Experimental setup for proposed time domain SPE/DPSK OCDMA scheme

The inset (i) and (ii) in Fig. 2 show the spectrum of the original 10GHz and generated 2.5GHz optical pulse trains, respectively. An optical band-pass filter is then used to cut the input spectrum into  $\sim 1.5$ nm spectral range. In the time domain SPE and DPSK data modulation section, a reverse dispersion fiber (RDF) is used to provide a negative dispersion ( $-312.5$ ps/nm) and stretch the input optical pulse. Different spectral components will spread at different positions in time domain. A phase modulator driven by combining 8-chip, 20Gchip/s optical code patterns (corresponding to 8-chip 20GHz/chip spectral code patterns) and 2.5Gbps DPSK data then phase modulate the stretched optical pulse. To accurately synchronize the optical code pattern and stretched pulse, a tunable optical delay line is employed before the phase modulator, so the optical code pattern can precisely modulate the phase of corresponding spectral component. After the phase modulation, a span of 34 km single mode fiber (SMF) is used to compress the stretched optical pulse and generate the DPSK data modulated SPE signal. The SMF functions as the transmission fiber as well. The dispersion of the whole transmission system is managed globally by utilizing another piece of dispersion compensation fiber (DCF) to compensate the dispersion mismatch. The total dispersion of the SMF and DCF is approximately 312.5ps/nm.

To recover the original data, the generated SPE signal has to be spectral phase decoded and then DPSK demodulated. The spectral phase decoding is directly performed in spectral domain by utilizing an AWG based device or VBS with the complementary spectral code (OC) pattern. The channel spacing of the AWG or VBS is 10GHz, so two spectral lines of the spectral phase decoder correspond to one chip for the 8-chip, 20GHz/chip spectral code pattern. After the spectral phase decoding, the auto-correlation signal is directed into a 2.5GHz DPSK demodulator followed by a balanced detector to recover the original data. A 2.65GHz low pass filter is used after the balanced detector to perform data-rate detection. The regenerated data and

2.5GHz clock signal from a clock and data recovery (CDR) circuit are then forwarded to an error detector to measure the bit-error-rate (BER) performance.

In the experiment, the dispersion of the RDF is one of the key factors to affect the final decoding performance. Figures 3(a) - 3(c) show the calculated decoded waveforms for the RDF with dispersion of  $-270.5\text{ps/nm}$ ,  $-300.5\text{ps/nm}$  and  $-340.5\text{ps/nm}$ , respectively. The deviation of the fiber dispersion from the ideal value will result in lower peak intensity and relatively higher sidelobes due to the mismatch of the corresponding spectral code with that in the spectral phase decoder. Figure 3(d) shows the calculated peak to wing ratio (P/W) of the correctly decoded waveform for different dispersion value, from which one can see the P/W can reach up to  $\sim 63$  for the dispersion of  $-312.5\text{ps/nm}$  but it will be degraded as the dispersion deviation increases.

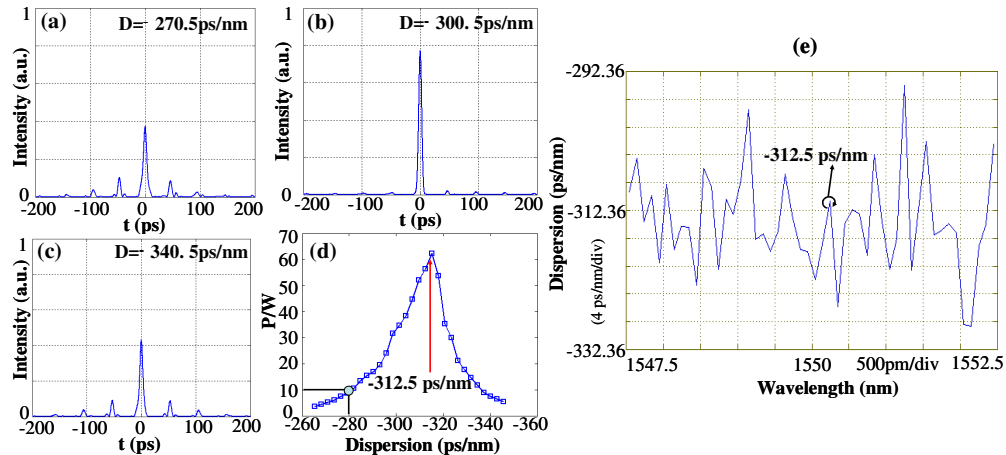


Fig. 3. (a) Decoded waveform for dispersion of  $-270.5\text{ps/nm}$ ; (b) Decoded waveform for dispersion of  $-300.5\text{ps/nm}$ ; (c) Decoded waveform for dispersion of  $-340.5\text{ps/nm}$ ; (d) Peak to wing ratio versus RDF dispersion and (e) Measured dispersion of the RDF used in the experiment.

For the dispersion of  $-312.5\text{ps/nm}$ , the 8-chip,  $20\text{Gchip/s}$  ( $50\text{ps/chip}$ ) optical code pattern corresponds to exactly 8-chip,  $20\text{GHz/chip}$  spectral code pattern, so the spectral phase decoder with channel spacing of  $10\text{GHz}$  can be used to effectively decode the encoded SPE signal, while for the other dispersion values, the spectral code pattern deviate from the  $20\text{GHz/chip}$  leading to higher sidelobes in the decoded waveform. The requirement of the dispersion deviation is not very strict, for  $P/W = 10$ , the deviation tolerance is about  $\pm 32.5\text{ps/nm}$ , which can be easily maintained in the system. Figure 3(e) shows the measured chromatic dispersion of the RDF used in the experiment. The dispersion of the RDF is approximately  $-312.5\text{ps/nm}$  at  $1550.28\text{nm}$  which guarantees the feasibility of decoding using the spectral phase decoder with  $10\text{GHz}$  channel spacing.

For the RDF with dispersion of  $-312.5\text{ps/nm}$ ,  $1.28\text{nm}$  ( $\sim 160\text{GHz}$ ) spectral range will spread within the whole bit duration of  $400\text{ps}$ , therefore, the original optical pulse with  $4\text{ps}$  pulse width covering  $\sim 3.5\text{nm}$  spectral range will generate significant overlap between two adjacent stretched pulses which will degrade the decoding and transmission performance. Figure 4 shows the peak to wing ratio (P/W) and peak intensity of the decoded pulse versus the light pulse width for code: 10101010.

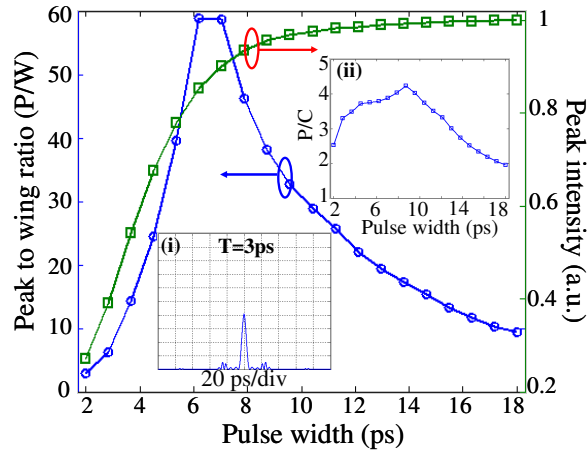


Fig. 4. Peak to wing ratio (P/W) and peak intensity versus light pulse width. The inset (i) is the decoded waveform for pulse width of 3ps. The inset (ii) shows the average power contrast ratio (P/C) versus the pulse width.

As the light pulse width decreases from 6ps, the decoding performance gradually degrades with lower P/W and peak intensity. The inset (i) in Fig. 4 shows the decoded waveform for light pulse width of 3ps, from which one find that the decoded waveform has large sidelobes and low peak intensity. This is mainly because each stretched optical pulse exceeds one bit period of 400ps inducing significant overlap between two adjacent stretched pulses in time domain. The overlapped spectral components will be phase modulated by other code patterns that cannot be correctly decoded by the spectral phase decoder and thus generate large sidelobes in the decoded waveform which directly lower the P/W and peak intensity. On the other hand, when the pulse width increases from 8ps, the stretched pulse can no longer cover the whole bit period, so the effective code length will gradually decrease resulting in the degradation of the P/W. The average power contrast ratio (P/C) between the auto-/cross -correlation versus the light pulse width is also shown in the inset (ii) in Fig. 4, from which one can see that the P/C exhibit the similar trend as the P/W. Too narrower or wider laser pulse will degrade both the P/W and P/C. To address this issue, a suitable optical bandpass filter is an essential component in the proposed scheme to cutoff the wing spectrum of the ultra-short optical pulse to reduce the overlap. In the experiment, we employ two cascaded optical band-pass filters with 3dB bandwidth of 2nm but different center wavelength before the RDF to cut off the residual input spectrum to reduce the overlap between two adjacent stretched pulses and improve the decoding performance. Figures 5(a) and 5(b) shows the spectrum and waveform of the stretched pulse after the cascaded BPFs, respectively. As shown in Fig. 5(a), the original spectrum has been cut by the BPFs into 1.5nm spectral range corresponding to the light pulse width of ~8ps. The adjacent stretched pulses have no obvious overlap due to the relatively lower intensity of the wing spectrum, which can be seen from Fig. 5(b).

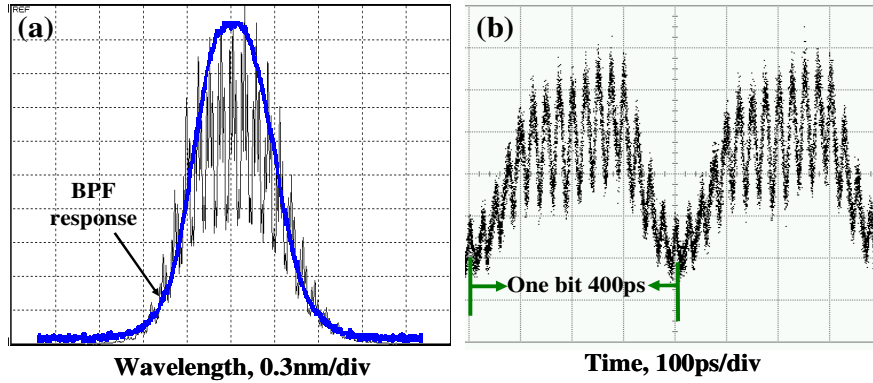


Fig. 5. (a) Input spectrum before RDF (the solid blue line is the spectral response of the cascaded BPFs) and (b) waveform of two adjacent stretched optical pulses

The timing error between the optical code pattern and stretched pulse also has significant effect on the decoding performance. The P/W versus the timing error ( $T_d$ ) is depicted in Fig. 6, from which one find that the P/W gradually decreases from 63 to 0 as the timing error increases from 0 to 20ps. The two insets in Fig. 6 are the decoded waveforms for timing error of 2ps and 10ps, respectively. For the inset (i), the decoded waveform still has high peak intensity while for the inset (ii), large sidelobes appear in the decoded waveform. The timing error corresponds to wavelength mismatch in the experiment. When the timing error increases, the code pattern will modulate the phase of different spectral components resulting in phase error in the spectral phase decoder, and thus the decoding performance will be significantly degraded. For a P/W of 10, the tolerance of timing error is  $\sim 4.5$  ps. A commercial available tunable optical delay line with tuning range of  $\sim 400$ ps (one bit period) and delay resolution of 0.2ps is used to accurately control the timing error.

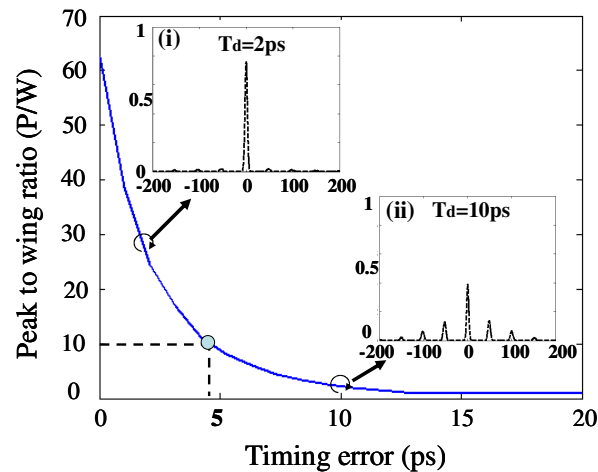


Fig. 6. Peak to wing ratio (P/W) versus timing error between the code pattern and stretched pulse

## 4. Encoding/decoding experiment

### 4.1 Array-waveguide-grating (AWG) based en/decoding

We have carried out an encoding/decoding experiment using AWG based device for spectral phase decoding. The AWG device has 21 channels and spectrally centers at 1550.28nm with 10GHz channel spacing. It can control the amplitude and phase of each channel individually. Four different binary phase shift keying (BPSK) optical code patterns: 10101010, 11101000, 11100100 and 00100010 have been used in this demonstration. Figure 7(a) shows the decoded waveform for the four codes using the AWG device. All the four codes have been decoded with high auto-correlation peak pulse and several sidelobes. The existing of the sidelobes is mainly due to the non-smooth Gaussian-shape spectral response of the AWG device and the errors in controlling the amplitude and phase of the AWG device. The AWG device is polarization dependent, so the amplitude and phase of each channel is very sensitive to the polarization change of the input optical signal. The phase control in the AWG device is also related to the relative phase shift of the two adjacent spectral channels. The phase error in the initial channels will be accumulated in the latter channels resulting significant degradation of the decoding performance. Figure 7(b) shows the cross-correlation signal for OC1 with the other codes.

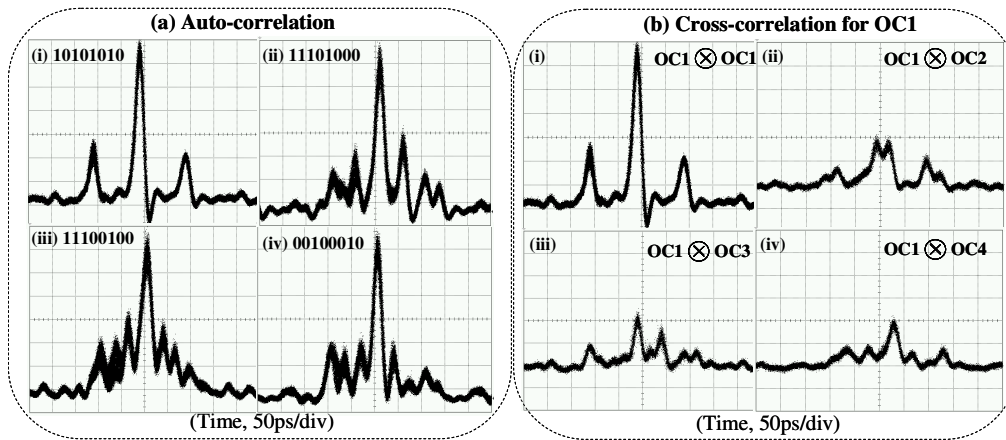


Fig. 7. (a) Auto-correlation signal for four optical codes: 10101010, 11101000, 11100100 and 00100010, respectively. (b) Cross-correlation signal for OC1 with the other codes.

The power contrast ratio (P/C) between the auto-/cross -correlation is about 2 which can be further improved by using decoders with more smooth spectral response and more accurate phase control.

### 4.2 Variable-Bandwidth-Spectrum-Shaper (VBS) based en/decoding

To effectively improve the decoding performance, a Variable-Bandwidth-Spectrum-Shaper (VBS), which is composed of grating, lens, spatial light modulator (SLM) and reflector, is used as the decoder in the experiment. The VBS can synthesize arbitrary optical spectrum and waveform with the advantages of high-precision amplitude and phase control, polarization independent, compactness and low-insertion loss [22]. The spectral phase decoding can be directly performed in spectral domain by utilizing the VBS with complementary spectral code (OC) pattern. The VBS used in the experiment can control the amplitude and phase with high resolution in the wavelength region covering the entire C band. The amplitude and phase control in VBS is very straightforward, which only need to adjust the absolute value instead of the relative value in the AWG. The amplitude control range is 30dB with a fluctuation of 0.1dB,

and the phase control range is  $2\pi$  with a resolution of  $0.04\pi$  [23]. The VBS has 340 control channels with channel spacing of 10GHz. Seven different BPSK optical code patterns, OC1~OC7: 11110000, 11001100, 10101010, 1110100, 11100100, 10101100 and 00100010 have been used in the encoding/decoding experiment.

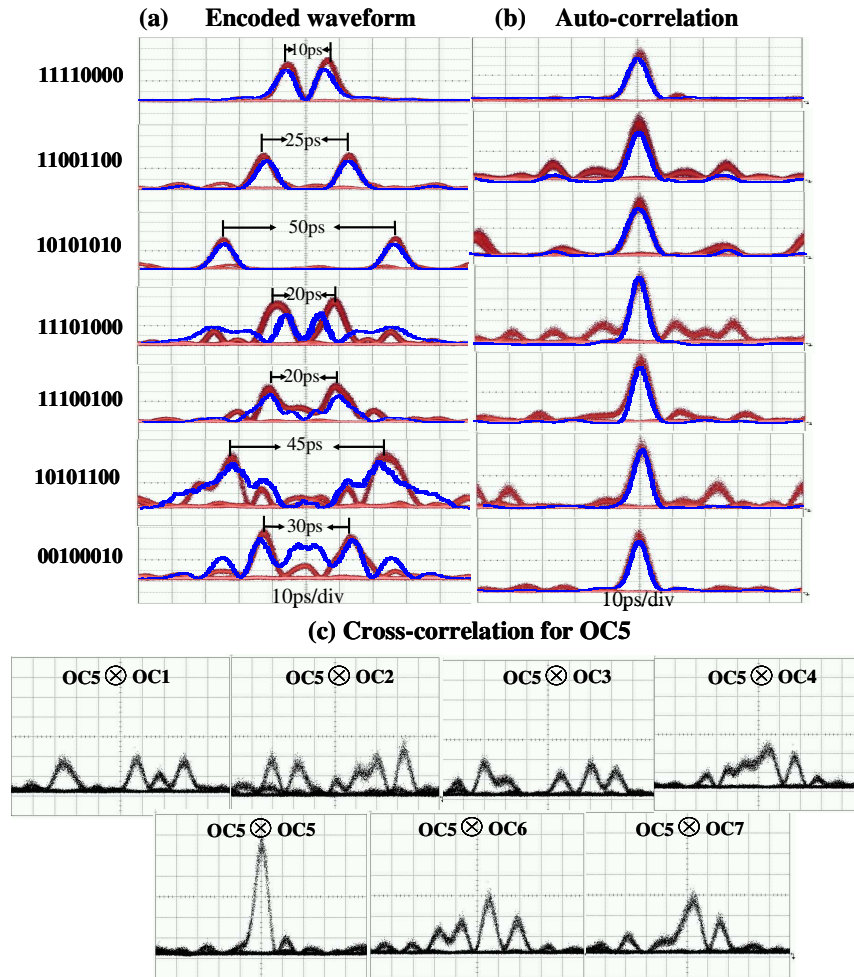


Fig. 8. (a) Encoded waveform and (b) decoded waveform of experimental (solid red line) and simulated results (solid blue line) for codes OC1~OC7. (c) Cross-correlation signal for OC5.

The measured encoded and decoded waveforms using an optical sampling oscilloscope (solid red lines), and simulated results (solid blue lines) are shown in Figs. 8(a) and 8(b), from which one can see that the encoded and decoded waveform of the first three codes agree well with the simulated results. For the other four codes, the profile of the encoded waveform also matches with our simulated results though the detail of the waveform has a little deviation generally due to the code transition from the pulse pattern generator and the limited resolution of the optical sampling oscilloscope. Compared with the AWG decoding results, the VBS exhibits excellent decoding performance for all the seven codes as can be seen from the auto-correlation signal in Fig. 8(b) though there are still a few sidelobes which can be partially ascribed to non-ideal phase control generated by the crosstalk of the VBS. Figure 8(c) shows the waveform of cross-correlation signal for OC5, from which we can see the power contrast ratio

is  $\sim 2$  due to the limited code length. The discrimination of different codes can be realized by proper optical thresholding.

### 5. SPE/DPSK data modulation using single PM and 2.5Gbps transmission experiment

We have carried out a proof-of-principle experiment with the proposed scheme for simultaneously generation of time domain SPE and 2.5Gbps DPSK data modulation with 8-chip, 20Gchip/s optical code patterns using single phase modulator. The spectral phase decoding has been performed by using the VBS based spectral decoder. A fixed data pattern with  $2^7-1$  pseudo random bit sequence (PRBS) was used in this experiment. The original data 1111110011 11...was precoded into DPSK data format and then mixed with the optical code pattern to drive the phase modulator. The decoded waveform using the VBS for OC5 is shown in Fig. 9 (a), from which one can see that the decoded pulses have similar waveform but different phases according to the DPSK data. In this case, the phases are  $000000\pi 00000\pi\dots$ , respectively. After the 2.5GHz DPSK demodulator and balanced detector, the original data pattern has been recovered as 111111001111...whose waveform is shown in Fig. 9 (b). The corresponding eye diagram with clear eye opening is also shown in Fig. 9(c). The DPSK demodulation has no obvious degradation because of the spectral phase decoding. Figure 9(d) shows the measured BER performance together with the eye diagram after 34km transmission using the 2.5Gbps  $2^7-1$  PRBS data for all the codes.  $BER < 10^{-9}$  and clear eye opening have been successfully achieved for all the codes. The difference of power penalty indicates the different decoding performance of each code.

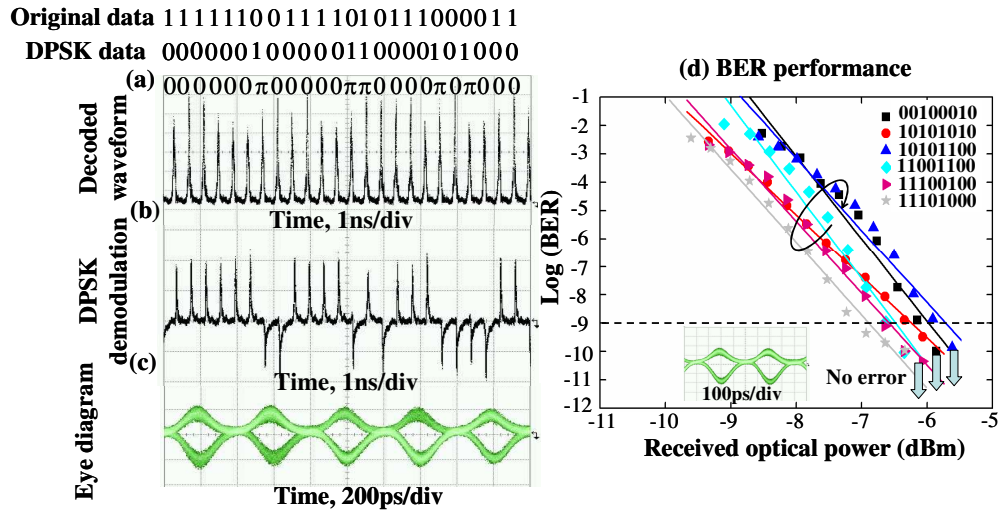


Fig. 9. (a) Decoded waveform; (b) Demodulated DPSK data; (c) Eye diagram and (d) BER performance for  $2^7-1$  PRBS data with different codes

The successful 2.5Gbps DPSK data transmission verifies the feasibility of our proposed modulation scheme that generate time domain spectral phase encoding and DPSK data modulation using single phase modulator, and decoding using a conventional spectral phase decoder in spectral domain. In the proposed scheme, the optical code pattern and DPSK data can be generated and reconfigured rapidly by programming the pulse pattern generator, therefore, the flexibility of our OCDMA system can be significantly improved, exhibiting the potential to enhance the network security.

## 6. Conclusion

We have proposed and experimentally demonstrated a time-domain spectral phase encoding scheme using single phase modulator for simultaneous generation of optical code pattern and DPSK data modulation. AWG and VBS have been used to perform spectral phase decoding directly in spectral domain. The effect of light pulse width, fiber dispersion and timing error between code pattern and stretched pulse on the decoding performance is theoretically discussed and verified in the experiment. 2.5Gbps DPSK data with 8-chip, 20GHz/chip optical code patterns have been generated using single phase modulator, decoded using a VBS and transmitted over 34km fiber with  $BER < 10^{-9}$ . The proposed scheme has very simple configuration and improved flexibility that can rapidly reconfigure the optical code. It exhibits the potential to improve the data confidentiality for optical code division multiple access (OCDMA) and secure optical communication applications.

## Acknowledgements

This work is partly supported by Royal Society International Joint Project. The authors would like to thank H. Sumimoto and Y. Tomiyama of NICT for their technical support in this experiment. Zhensen Gao also acknowledge the support of the International Travel Grant from the Royal Academy of Engineering.